Electronic Supplementary Information

Mechanical Path to a Photogenerated Structure: Ball Milling-Induced Phase Transition of a Gold(I) Complex

Kenta Sakurada, Tomohiro Seki, and Hajime Ito*

Division of Applied Chemistry and Frontier Chemistry Center (FCC), Fuculty of Engineering, Hokkaido University, Sapporo, Hokkaido 060-8628, Japan

hajito@eng.hokudai.ac.jp

Contents

1. General **S1**

2. Photophysical properties of 1 **S2**

3. Preparation of $1Y_G$ **S4**

4. NMR spectra and elemental analysis of 1 **S5**

6. Crystal structures of 1 **S7**

7. DSC and thermal profile of 1 **S10**

8. References **S11**

1. General

All commercially available reagents and solvents are of reagent grade and were used without further purification unless otherwise noted. Solvents for the synthesis were purchased from commercial suppliers, degassed by three freeze-pump-thaw cycles and further dried over molecular sieves (4 Å). NMR spectra were recorded on a JEOL JNM-ECX400P or JNM-ECS400 spectrometer (^{1}H: 400 MHz; ^{13}C: 99.5 MHz) using tetramethylsilane and $CDCl_3$ as internal standards, respectively. Emission spectra were recorded on a Hitachi F-7000 spectrometer. Fluorescence microscopic spectra were recorded on a Hamamatsu PMA-12 Photonic Multichannel Analyzer. The emission quantum yields of the solid samples were recorded on a Hamamatsu Quantaurus-QY spectrometer with an integrating sphere. Emission lifetime measurements were recorded on a Hamamatsu Quantaurus-Tau spectrometer. Elemental analyses and low- and high resolution mass spectra were recorded at the Center for Instrumental Analysis, Hokkaido University. Photographs were obtained using Olympus BX51 or SZX7 microscopes with Olympus DP72, Nikon D5100 or digital cameras. As strong UV light for photoinduced phase transition of **1**, an Olympus BX51 fluorescence microscope equipped with an Ushio 100 W ultrahigh-pressure mercury lamp USH-1030L and Olympus fluorescence mirror unit U-MWU2 (λ_{max} = 342 nm, 108 mW·cm^{-2}) was used. Power density of the UV light was measured on Hamamatsu UV power meter C6080-04 and C6080-385.

2. Photophysical properties of 1

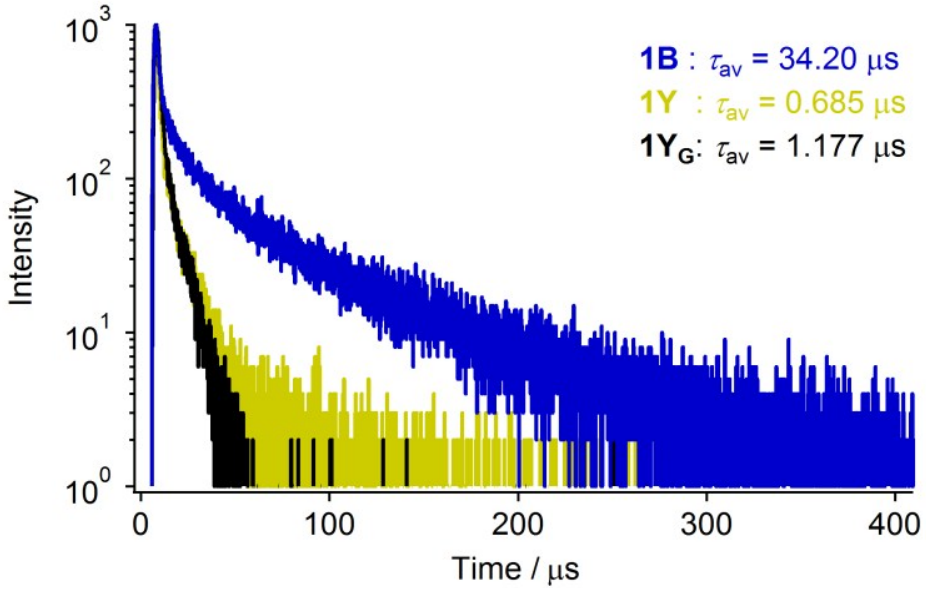

Fig S1 Emission decay profiles (λ_{ex} = 370 nm) of **1B** (blue line, λ_{em} = 485 nm), **1Y** (yellow line, λ_{em} = 580 nm), and **1Y$_G$** (black line, λ_{em} = 580 nm).

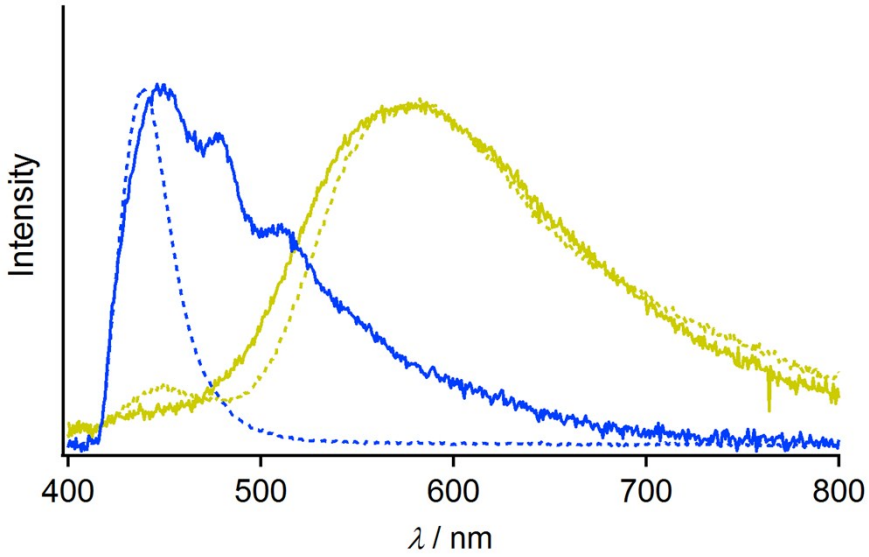

Fig. S2 Normalized emission spectra of **1B** (blue lines) and **1Y** (greenish yellow lines) at 303 K (solid lines) and 123 K (dotted lines) with an UV light at 367 nm with a power density of approx. 3 mW·cm^{-2}.

Table S1 Photophysical properties of **1B**, **1Y** and $\mathbf{1Y_G}$

	Φ_{em} / -	τ_{av} / μs[d,e] (λ_{em} / nm)	τ_1 / μs[d] (A / -)	τ_2 / μs[d] (A / -)	τ_2 / μs[d] (A / -)
1B	0.022[a]	34.2 (485)	0.292 (0.27)	5.839 (0.17)	59.079 (0.56)
1Y	0.005[b]	0.685 (580)	0.297 (0.79)	2.141 (0.21)	
$\mathbf{1Y_G}$	0.31[c]	1.177 (580)	0.954 (0.81)	2.128 (0.19)	

[a]λ_{ex} = 370 nm. [b]λ_{ex} = 390 nm. [c]λ_{ex} = 390 nm. [d]λ_{ex} = 370 nm. [e]$\tau_{av} = (A_1\tau_1 + A_2\tau_2 + \cdots) / (A_1 + A_2 + \cdots)$.

3. Preparation of $1Y_G$

The polymorph $\mathbf{1Y_G}$ was obtained by ball-milling (4600 rpm, 30 min) of **1B** or **1Y**. To prevent the chemical decomposition of the sample by mechano-generated heat, the sample was cooled to room temperature after every 5 min during the ball-milling process (5 min × 6). Temperature raise upon the ball-milling treatment for 5 min was 2.7 °C, indicating negligible influence of the heat on the phase transition from **1B** to $\mathbf{1Y_G}$.

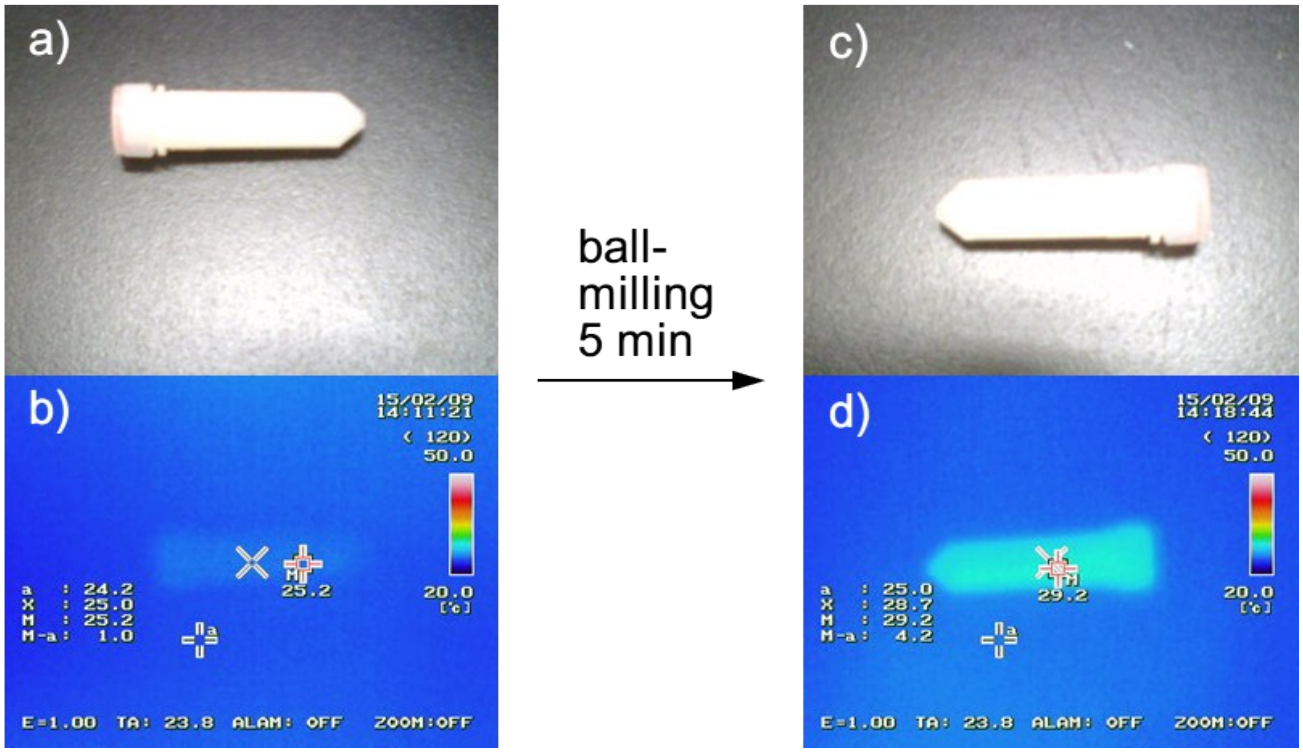

Fig. S3 Photographs (upper) and thermography (lower) of **1** in the ball-milling holder. a) Photographs of **1B** crystal in the ball-milling holder before grinding. b) Thermography of **1B** crystal in the ball-milling holder before grinding. c) Photographs of $\mathbf{1Y_G}$ powder in the ball-milling holder taken just after 5 min ball-milling. d) Thermography of $\mathbf{1Y_G}$ powder in the ball-milling holder taken just after 5 min ball-milling. Temperature raise upon ball-milling for 5 min. is 2.7 °C.

4. NMR spectra and elemental analysis of 1

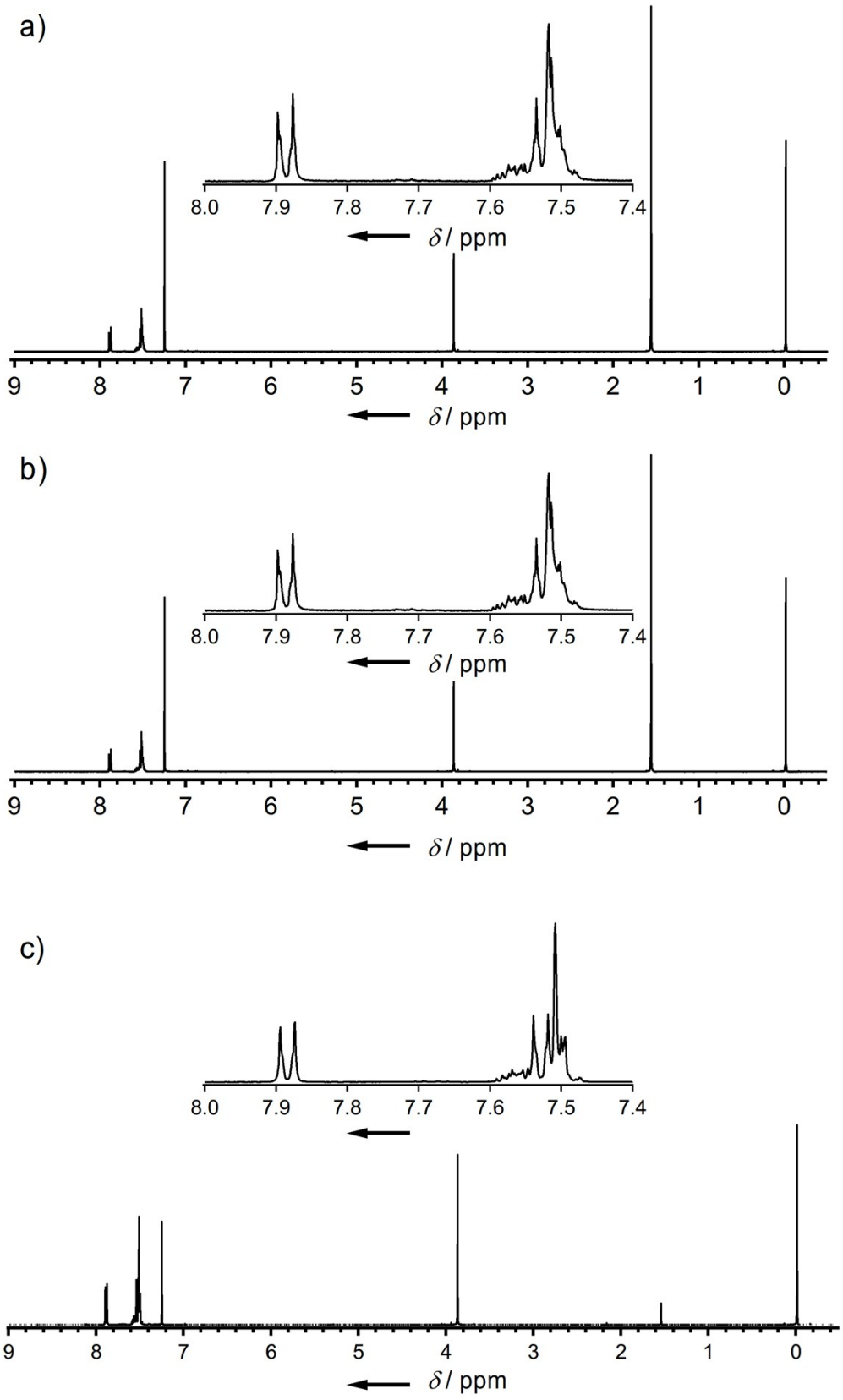

Fig. S4 ^{1}H NMR spectra of **1B** (a), **1Y** (b), and $\mathbf{1Y_G}$ (c) dissolved in $CDCl_3$.

Table S2 Elemental analyses of the polymorphs **1B**, **1Y**, and $\mathbf{1Y_G}$.

	C	H	N
Calculated for **1** ($C_{15}H_{12}AuNO_2$)	41.39	2.78	3.22
1B	41.34	2.81	3.21
1Y	41.32	2.82	3.23
$\mathbf{1Y_G}$	41.31	2.83	3.23

6. Crystal structures of 1

Single crystals structures of **1B** and **1Y** were already reported.[1]

Table S3 Summary of X-ray crystallographic data for **1B** and **1Y**.[1]

Polymorph	**1B**	**1Y**
CCDC Name	CCDC 987280	CCDC 987281
Empirical Formula	$C_{15}H_{12}AuNO_2$	$C_{15}H_{12}AuNO_2$
Formula Weight	435.23	435.23
Crystal System	triclinic	triclinic
Crystal Size / mm	0.171 × 0.115 × 0.037	0.171 × 0.115 × 0.037
a / Å	7.381(2)	6.0552(5)
b / Å	11.755(2)	7.0297(6)
c / Å	15.940(3)	15.969(2)
α / °	102.912(5)	96.315(3)
β / °	92.025(5)	93.979(3)
γ / °	100.595(5)	90.279(3)
V / Å^3	1320.8(4)	673.9(1)
Space Group	P-1 (#2)	P-1 (#2)
Z value	4	2
D_{calc} / g·cm^{-3}	2.189	2.145
Temperature / K	123	123
$2\theta_{max}$ / °	51.2	54.9
μ (MoK$_\alpha$) / cm^{-1}	111.729	109.488
No. of Reflections Measured	Total : 10450 Unique : 4756 (R_{int} = 0.1301)	Total : 5525 Unique : 2516 (R_{int} = 0.0574)
Residuals: R_1 (I > 2.00σ (I)) / %	8.67	5.42
Residuals: wR_2 (All reflections) / %	24.96	13.30
Goodness of Fit (GOF)	1.106	1.045
Maximum peak in Final Diff. Map / Å^3	2.44 e$^-$	5.16 e$^-$
Minimum peak in Final Diff. Map / Å^3	–3.78 e$^-$	–2.80 e$^-$

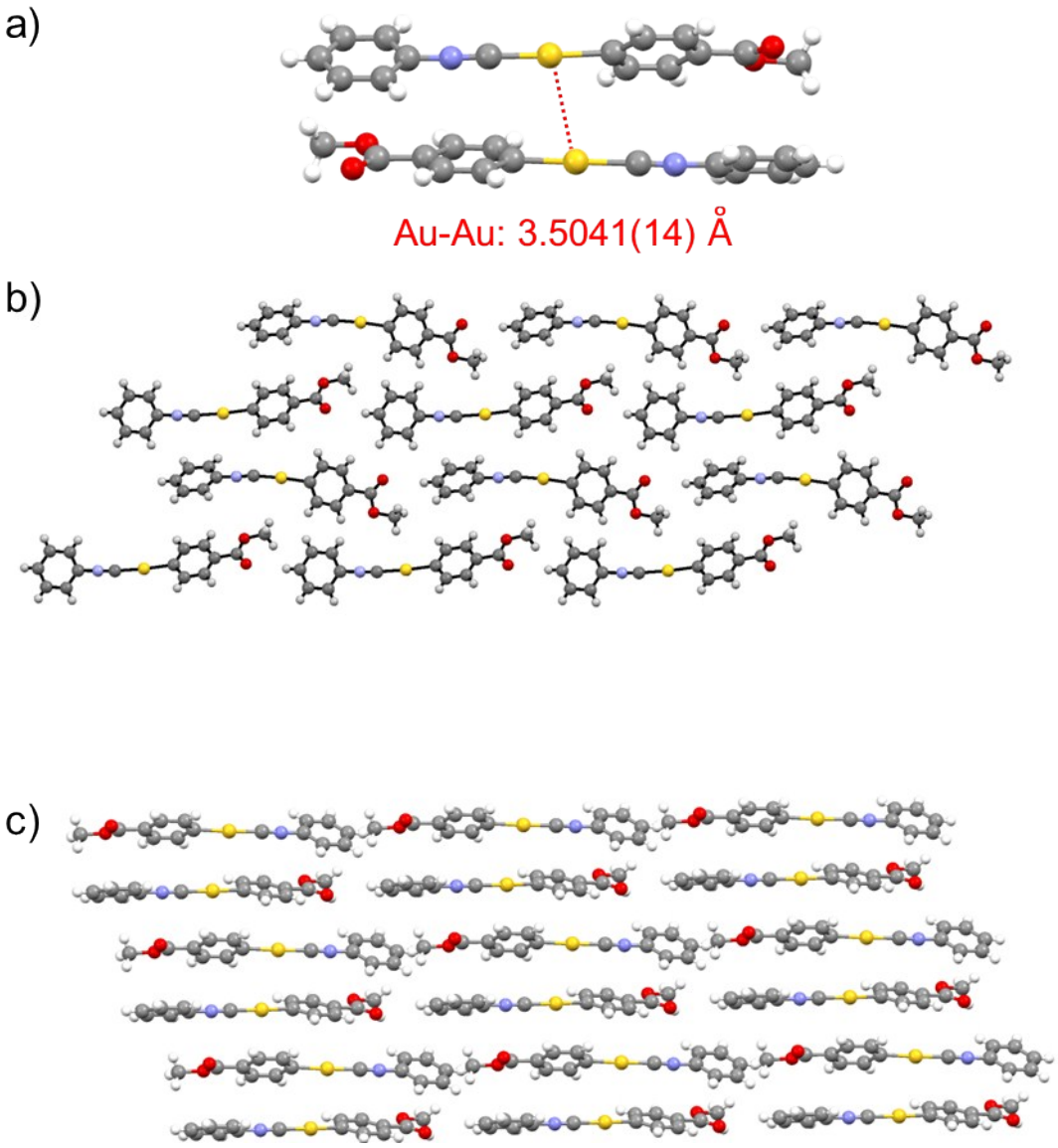

Fig. S5 Crystal structure of **1B**. a) The dimer unit in **1B** crystal. b) Packing structure of **1B** viewed along *a* axis. c) Packing structure of **1B** viewed along *c* axis. See ref. S1.

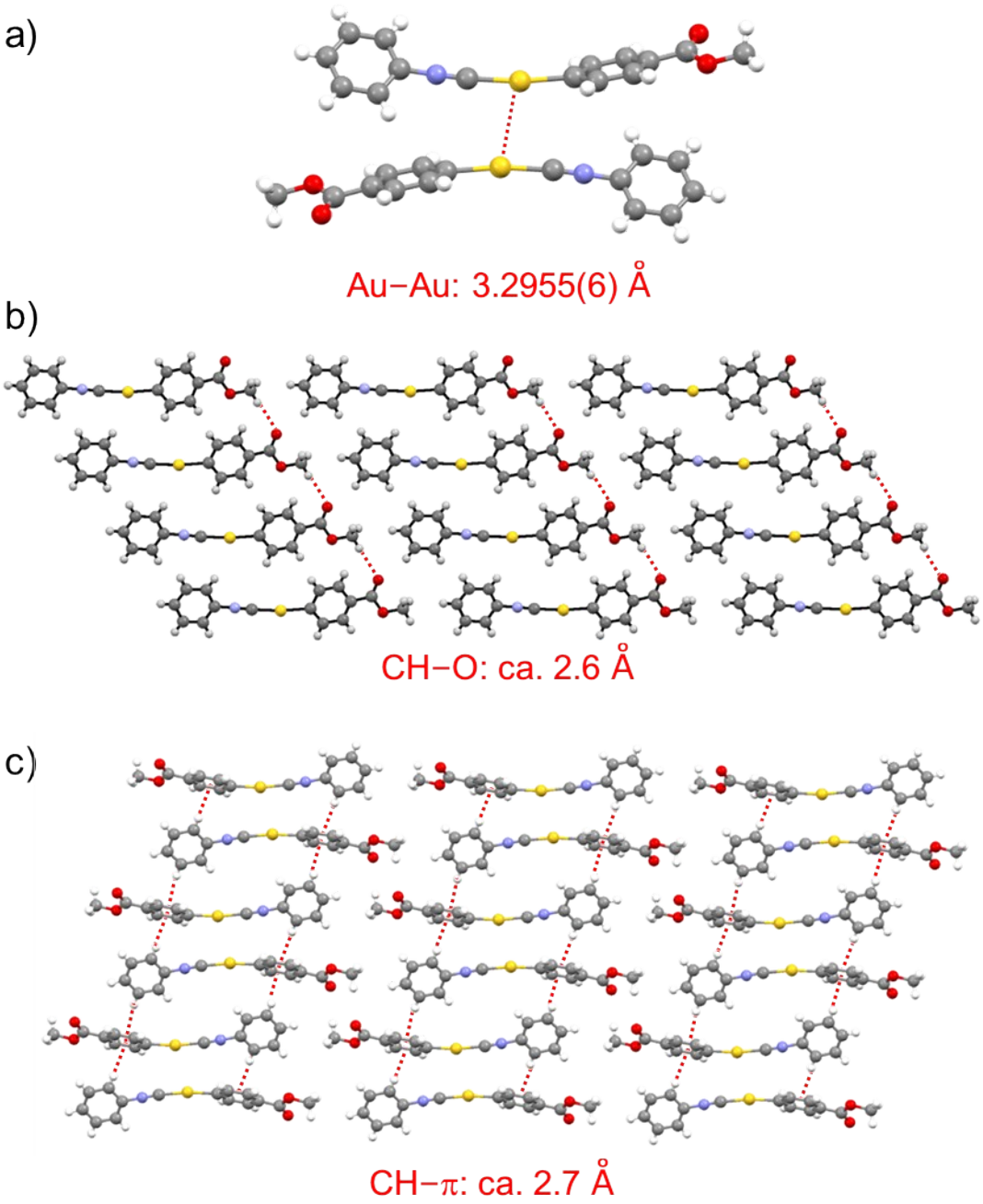

Fig. S6 Crystal structure of **1Y**. a) The dimer unit in **1Y** crystal. b) Packing structure of **1Y** viewed along *b* axis. c) Packing structure of **1Y** viewed along *a* axis. See ref. S1.

7. DSC and thermal analyses of 1

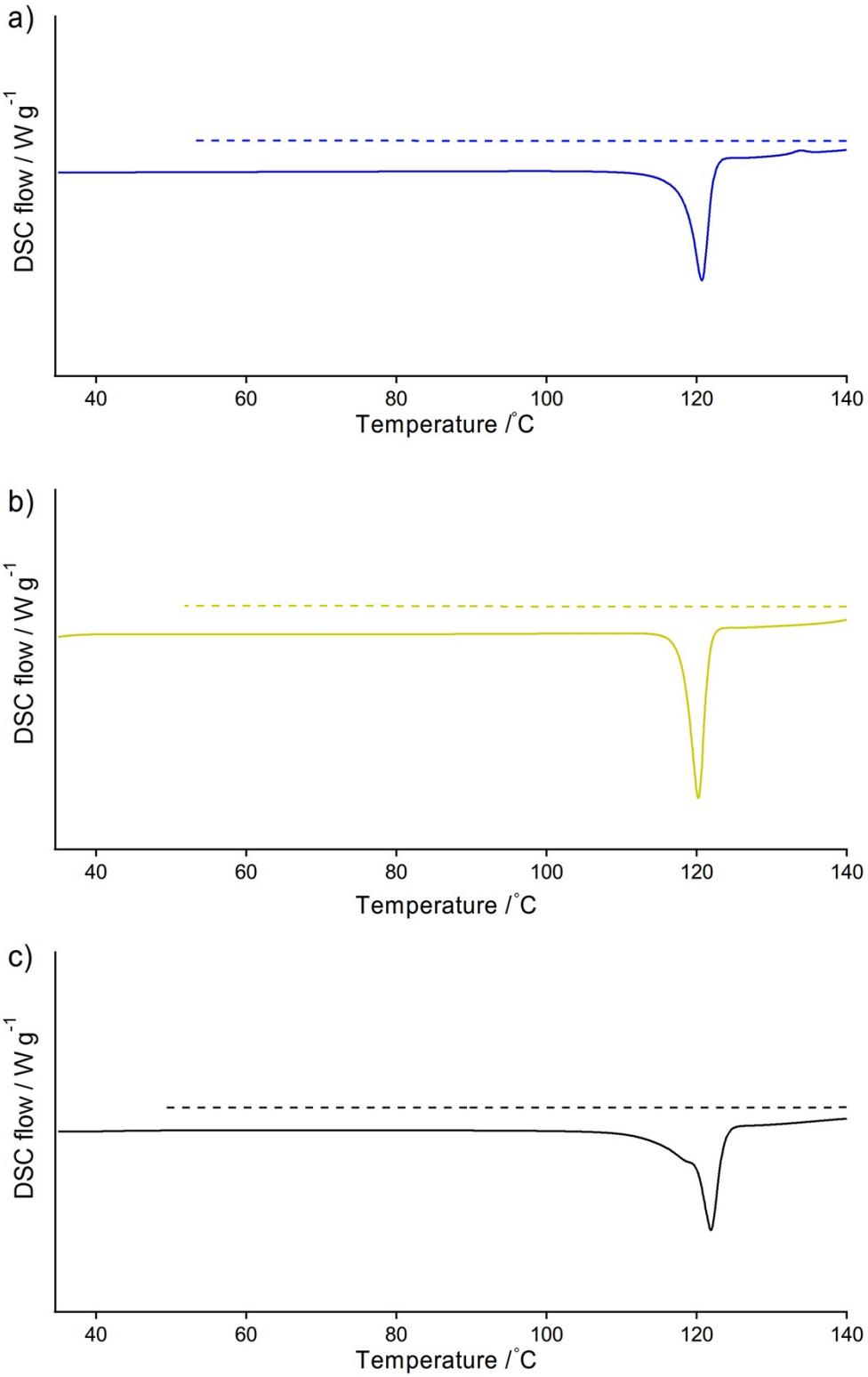

Fig. S7 DSC profiles of a) **1B** (blue line), b) **1Y** (yellow line), and c) $\mathbf{1Y_G}$ (black line) at heating (solid line) and cooling (dotted line) rates of 10 and 2 °C min^{-1}, respectively.

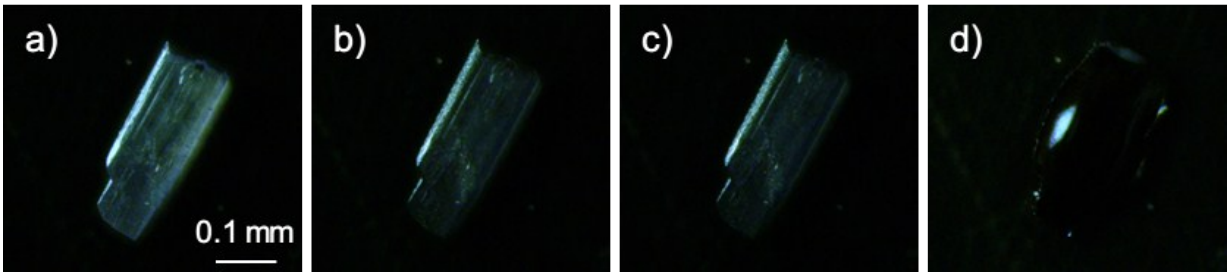

Fig. S8 Photographs of a **1B** crystal taken under UV irradiation (367 nm) at a) 30 °C, b) 60 °C, c) 90 °C, d) 120 °C. Intensity of the emission decreases thorough heating and the crystal melts at ca. 120 °C.

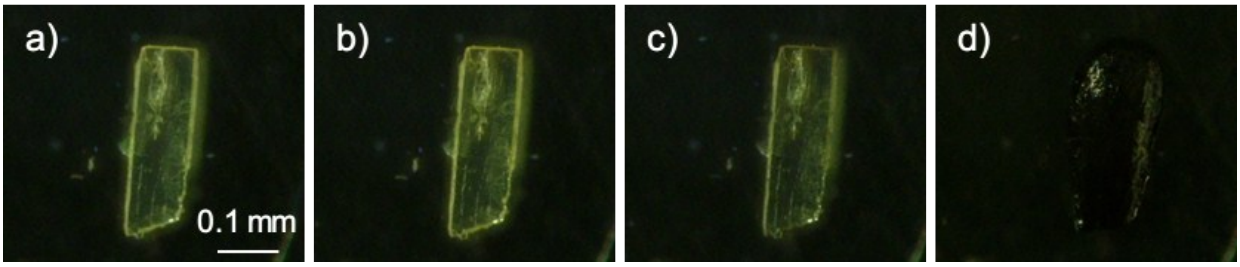

Fig. S9 Photographs of a **1Y** crystal taken under UV irradiation (367 nm) at a) 30 °C, b) 60 °C, c) 90 °C, d) 120 °C. Intensity of the emission decreases thorough heating and the crystal melts at ca. 120 °C.

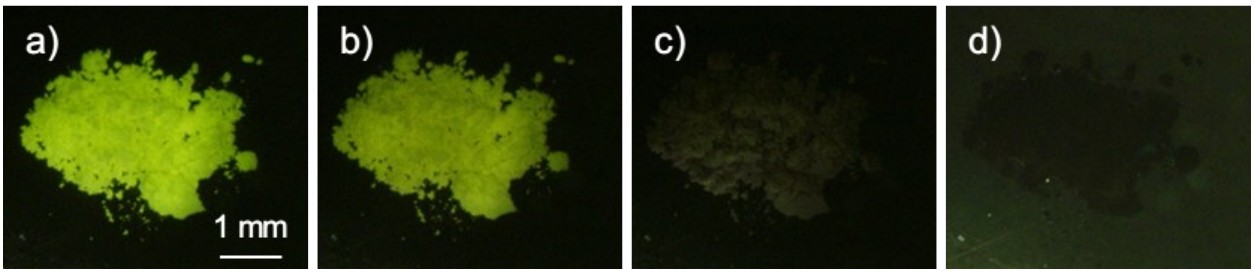

Fig. S10 Photographs of a $\mathbf{1Y_G}$ powder taken under UV irradiation (367 nm) at a) 30 °C, b) 60 °C, c) 90 °C, d) 120 °C. Intensity of the emission decreases thorough heating and the powder melts at ca. 120 °C.

8. References

1. T. Seki, K. Sakurada, M. Muromoto, H. Ito *Chem. Sci.*, **2015**, *6*, 1491-1497.